Ethanol Decomposition in Supercritical Water: An Operating Parametric Experimental and Kinetic Study

Liang Zhao,[a,*] Yuhang Yang,[a] Hongfang Zhou,[a] Zhengle Que,[a] and Yadi Pan [a,b]

Ethanol is an intermediate of the supercritical water decomposition of lignocellulosic biomass or biomass-derived compounds. In this study, experiments on ethanol decomposition in supercritical water were performed at different reaction temperatures (500 °C to 600 °C), residence times (6 s to 12 s), and initial ethanol concentrations (0.05 mol·L^{-1} to 0.20 mol·L^{-1}). Temperature had larger impacts on the ethanol conversion than the other factors. Higher temperatures and feedstock concentrations facilitated gas production. In addition, the higher temperature promoted the scissions of C-C and C-O bonds of ethanol. However, longer residence times did not improve the yields of H_2, CO, and C_2. Because the H_2-to-CO_2 ratio was much greater than 1, the water-gas shift reaction was not the dominant route during the ethanol conversion process. Further, the mechanism and kinetic model of ethanol supercritical water decomposition were proposed. The kinetics revealed that ethanol gasification in supercritical water was mainly dominated by ethanol dehydrogenation, the hydrogenation of intermediates, and the coke formations of CO and CH_4. In addition, H_2 was mainly formed *via* ethanol dehydrogenation and consumed *via* the hydrogenation of intermediates. The rate of coke formation was relatively low during ethanol decomposition.

Keywords: Ethanol; Supercritical water; Decomposition; Kinetics

*Contact information: a: College of Materials Science and Engineering, Nanjing Forestry University, Nanjing 210037, China; b: Co-Innovation Center of Efficient Processing and Utilization of Forest Resources, Nanjing Forestry University, Nanjing 210037, China; *Corresponding author: zl_06@126.com*

INTRODUCTION

During biomass gasification in supercritical water, many intermediates are produced, including carbohydrates, phenols, furfurals, acids, alcohols, and aldehydes. Based on the characterization analysis using the gas chromatography-mass spectrometer (GC-MS) and the Fourier transform-infrared (FT-IR) spectrometer, Durak (2015; 2018) and Genel *et al*. (2016) confirmed that the above-mentioned organics were detected in the liquid products of the biomass thermochemical conversion. Studies on the typical decomposition of intermediates are among the most effective technical routes for determining the biomass conversion mechanisms in supercritical water. Alcohols (methanol (Reddy *et al*. 2016), ethanol (Abdullah and Croiset 2014), 1-propanol (Chakinala *et al*. 2013), and glycerol (Reddy *et al*. 2016)) were detected during the degradation of lignocellulosic biomass or biomass-derived compounds in supercritical water. Small molecule intermediates, such as methanol and ethanol, are important intermediate compounds that can easily become converted into gas products under the appropriate reaction conditions (Chakinala *et al*. 2013). In addition, compared to the gasification of aldehydes (formaldehyde and acetaldehyde) and acids (formic acid and acetic acid) in supercritical water, the gasification efficiencies of methanol and ethanol are

usually lower (Chakinala *et al*. 2013; Zhao 2013). Therefore, it is necessary to further investigate the decomposition of small-molecule alcohols to achieve higher gasification efficiency for biomass gasification in supercritical water.

Castello *et al.* (2015) examined the reaction mechanism of glucose decomposition at 400 °C and reported that methanol can be produced *via* decarbonylation of glycoladehyde, self-disproportionation of formaldehyde, cross-disproportionation, and glycolic acid conversion. Methanol is the simplest alcohol with a relatively low reactivity, even at 600 °C and 25 MPa (gasification efficiency < 2 wt%) (Zhao 2013). The radical propagation reaction mechanism (Castello and Fiori 2012) is usually used to explain methanol decomposition in supercritical water. Chakinala *et al*. (2013) found that formic acid and formaldehyde are the key intermediates of methanol decomposition, and the formations of formic acid and formaldehyde are the controlling steps during the methanol gasification process in supercritical water. Further, some detailed kinetic models of methanol gasification in supercritical water have been well studied to reveal the degradation mechanism (Castello and Fiori 2012).

Ethanol fermentation from biomass is regarded as the main ethanol production technology of biomass conversion (Mesa *et al.* 2020). In supercritical water, the main purpose of feedstock gasification is hydrogen production (Kruse *et al*. 2010). Ethanol, as the feedstock in supercritical water, is more commonly derived from the residue of ethanol refineries (Sato *et al*. 2013). Arita *et al.* (2003) reported that acetaldehyde was obviously formed by ethanol dehydrogenation (Eq. 1), and ethylene coupled ethane were detected in the gas products (Eqs. 2 and 3). In addition, Chakinala *et al.* (2013) and Therdthianwong *et al.* (2011) deduced that some other trace compounds, such as acetone, 2-propanol, formaldehyde, and methanol, should exist in the liquid products of ethanol decomposition. At 380 °C to 516 °C and 31.5 MPa Hack *et al.* (2005) found that the Arrhenius-activation energy of ethanol decomposition is lower than that of methanol decomposition. This indicates that ethanol should be easier to gasify than methanol in supercritical water. Therdthianwong *et al*. (2011) also confirmed that the gasification efficiency of ethanol was approximately 18.3 wt% at 500 °C, 25 MPa, and 50 s residence time, which was higher than that of methanol (under 2 wt% (Zhao 2013)). Equations 1 through 3 are as follows:

$$CH_3CH_2OH \rightarrow CH_3CHO + H_2 \quad (1)$$

$$CH_3CH_2OH \rightarrow C_2H_4 + H_2O \quad (2)$$

$$C_2H_4 + H_2 \leftrightarrow C_2H_6 \quad (3)$$

Ethanol is an intermediate during lignocellulosic biomass decomposition in supercritical water and a reasonable resource for syngas production (Pinkard *et al.* 2019). Compared to methanol decomposition in supercritical water, the gasification mechanism of ethanol degradation process is more complex, and past reports on ethanol gasification were not thorough enough to clarify and control the supercritical water gasification of ethanol. The modeling of the kinetics at high pressures plays an important role in chemical process and has attracted research attention (Sangwan *et al*. 2015; Yan and Krasnoperov 2019). However, only a few studies were conducted at pressures high enough for more reliable determination of the kinetic parameters. In this study, several experiments and kinetic analyses on ethanol decomposition in supercritical water were conducted at different temperatures (500 °C to 600 °C), residence times (6 s to 12 s), and initial ethanol concentrations (0.05 $mol \cdot L^{-1}$ to 0.20 $mol \cdot L^{-1}$). Ethanol has not been well investigated as a potential hydrogen-production source. In this article, the studies on the effects of operating

parameters are conductive to better understand the ethanol conversion process in supercritical water. In addition, the present study of kinetics can be helpful to comprehensively reveal the thermochemical conversion mechanism of the ethanol decomposition. The experimental and kinetic study of the ethanol decomposition can also provide the research basis for further determining the raw biomass conversion mechanism in supercritical water.

EXPERIMENTAL

Reagents

In this study, ethanol (≥ 99.7 wt%) was purchased from Sinopharm Chemical Reagent Corporation (Shanghai, China). The distilled water was supplied by Nanjing Dongxinan Pure Water Corporation (Nanjing, China).

Apparatus and Procedures

The experiments were performed in a continuous reaction system (Fig. 1). The feedstock was pumped into the 2520 stainless steel coil reactor (Φ3 × 1 mm with a length of 13.35 m) by a high-performance liquid chromatography (HPLC) pump (FL2200; Fuli Instruments, Wenling, China). The coil reactor was heated by a tube electric furnace (7kW, VTL-1200; Yachi Instruments, Nanjing, China). After the reaction, the products of gasification were filtered through the two-stage filters (50 μm (first) and 5 μm (second), Swagelok, Shanghai, China). Then, *via* the back pressure valve (K956; Xiongchuan Technology, Beijing, China), the products of gasification were reduced to normal pressure. Finally, the gas and liquid products were separated by the gas-liquid separator (S4486; Aladdin Company, Shanghai, China). The gas products were collected with an aluminum foil air bag. Because the main purpose was to obtain hydrogen production by ethanol decomposition, these experiments mainly analyzed the gas products, which were analyzed *via* gas chromatography (GC) (Model 9790 Plus; Fuli Instruments, Wenling, China). Detailed analyses of liquid products were carried out later in the study. Based on the results of the experiments in this article, the fitting of dynamic equations was solved by Micromath Scientist (Micromath Company, version 3.0.0.215, Saint Louis, MO, USA).

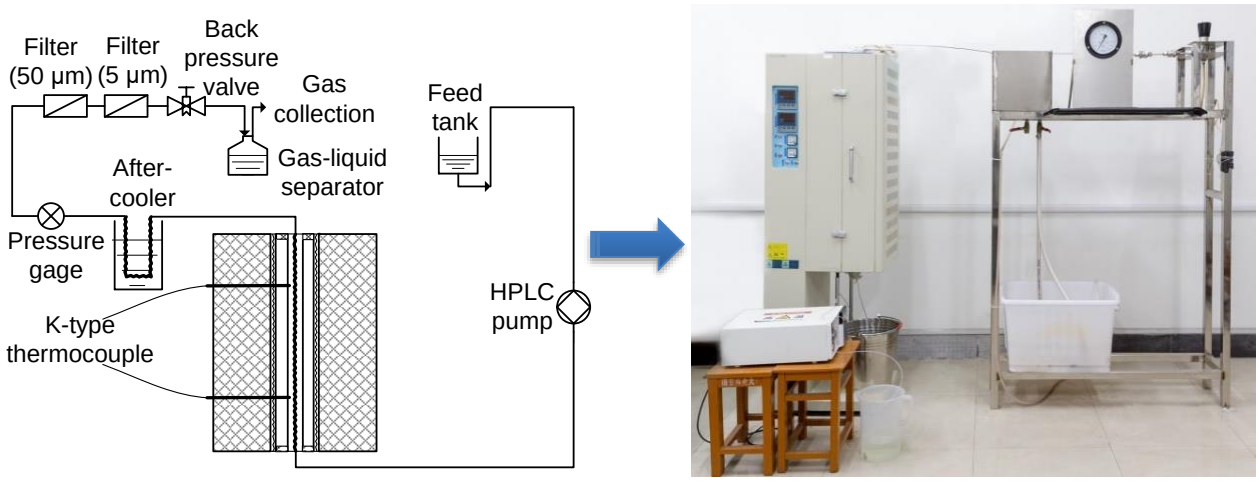

Fig. 1. A continuous reaction system

Due to the gasification efficiency of ethanol and the design parameters of this reactor (temperatures up to 600 °C and pressures of up to 30 MPa), the reaction temperature and pressure in this article were set at 500 °C to 600 °C and 23 MPa.

Data Interpretation

To analyze the ethanol gasification conversion in the experiments, the *GE* (gasification efficiency, wt%) and y_i (yields of each gas product, mol·kg^{-1}) were determined by Eq. 4 and Eq. 5, respectively,

$$GE = \left(\frac{\sum_i \frac{x_i \times 0.01 \times V \times M_i}{1000 \times 22.4}}{\frac{44.05 \times c_0 \times F}{1000}} \right) \times 100\% \tag{4}$$

$$y_i = \frac{x_i \times 0.01 \times V \times 1000}{22.4 \times 44.05 \times c_0 \times F} \tag{5}$$

where, x_i is the volume content of each gas product (vol%), M_i is the molar mass of each gas product (g·mol^{-1}), V is the yield of gas products (mL·min^{-1}), c_0 is the initial acetaldehyde concentration in the feedstock (mol·L^{-1}), and F is the mass flow rate of the feedstock (g·min^{-1}).

RESULTS AND DISCUSSION

The GC analysis of gas products showed that there were large amounts of H_2, CO, CO_2, CH_4, C_2H_6, and C_2H_4 and a small quantity of C_3H_6 (propene) in the gas products of ethanol decomposition in supercritical water at 500 °C to 600 °C. The starting compound ethanol was not detected in the gas products by the GC analysis. The yields of C_2-C_3 (C_2H_6, C_2H_4, and C_3H_6) during ethanol decomposition were higher than those of methanol (Boukis *et al*. 2006). As the components of C_2-C_3 were formed by the scission of the C-O bond (Chakinala *et al*. 2013), this indicates that the C-O bond was easier to break during ethanol decomposition than during methanol decomposition.

Temperature

According to Lee *et al.* (2002) (glucose, 480 °C to 750 °C), Zhao *et al*. (2020) (acetaldehyde, 500 °C to 600 °C), and Guo *et al.* (2012) (glycerol, 445 °C to 600 °C), reaction temperature is a key parametric factor in the decomposition of organic compounds in supercritical water. Therdthianwong *et al*. (2011) preliminarily performed ethanol decomposition at 500 °C to 600 °C and the relatively long residence time of approximately 50 s, and their results showed that the yields of C_2-C_3 were so low that they can be ignored. However, the pretest experiments in this study with short residence times of 6 s to 12 s found that the C_2-C_3 yields were considerable. Therefore, it is important to reveal the conversion mechanism of the decomposition of intermediates at shorter residence times (such as glucose at 425 °C to 600 °C with a residence time of 5.1 s to 9.9 s) (Holgate *et al*. 1995)). In this section, the reaction temperature was set at 500 °C to 600 °C, and the residence time was 12 s.

The yields and *GE* at different reaction temperatures are shown in Fig. 2. As shown in the figure, when temperatures increased from 500 °C to 600 °C, the gas product yields were dramatically increased, especially from 550°C to 600 °C. The reason is that the gas production of ethanol decomposition in supercritical water was dominated by free-radical reactions (Chakinala *et al*. 2013). Watanabe *et al.* (2004) reported that high reaction temperature (> 550 °C) favors free-radical reactions. Thus, from 550 °C to 600 °C, the *GE* value noticeably increased. Figure 2 shows that H_2 was the main component in the gas products. The H_2 yield at 600 °C was approximately 10 times as much as that at 550 °C. The H_2 production was likely promoted by the higher temperature *via* ethanol dehydrogenation (Eq. 1), reforming of long-living intermediates (acetaldehyde, methanol, *etc.*), and a water-gas shift reaction (Therdthianwong *et al*. 2011). In contrast to methanol, the C-C bond cleavage of ethanol is the characteristic reaction pathway that is favorable at high reaction temperatures (Kruse and Gawlik 2003). Therefore, increased reaction temperatures enhanced the yields of C_1 gas products (CO, CO_2, and CH_4) (Fig. 2a). The yields of C_2 gas products (C_2H_4 and C_2H_6) obviously increased as reaction temperature increased (Fig. 2b), which indicated that the higher reaction temperature facilitated the C-O bond scission. Because C_2H_4 was the precursor of C_3H_6 (as shown in Eq. 3) (Arita *et al*. 2003), the C_3H_6 yield in Fig. 2b indicated that the effect of reaction temperature (500 °C to 600 °C) on C_3H_6 production was relatively limited.

Therefore, higher reaction temperature was beneficial to ethanol gasification in supercritical water. To achieve high gas yields and gasification efficiency, the reaction temperature of ethanol decomposition should be above 550 °C.

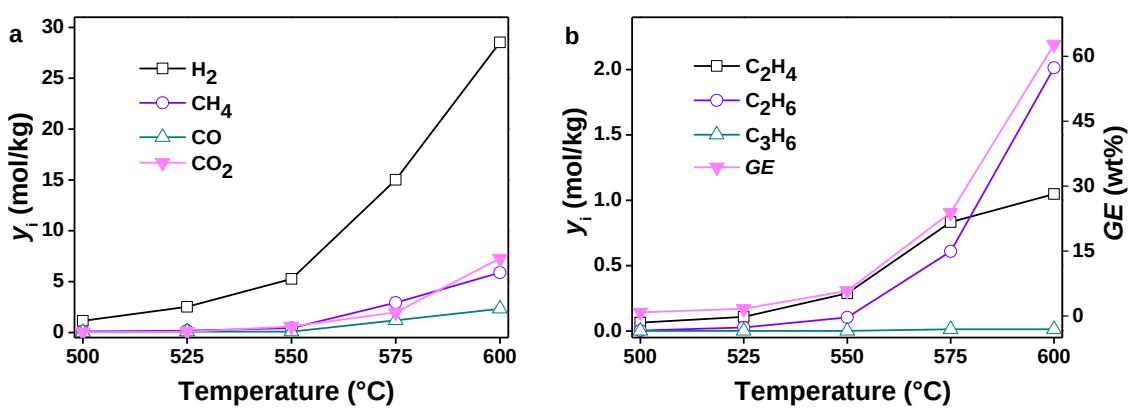

Fig. 2. Gas product yield and *GE* at different reaction temperatures (reaction pressure: 23 MPa, residence time: 12 s, and $[C_2H_5OH]_0$: 0.1 mol/L): (a) H_2, CH_4, CO, and CO_2; (b) C_2H_4, C_2H_6, C_3H_6, and *GE*

Residence Time

Based on the results in the previous section and the maximum service temperature of the reactor, the reaction temperature in this section was kept at 550 °C. The residence time range largely depends on the performance of the HPLC pump (flow rate range: 0.000 $mL \cdot min^{-1}$ to 9.999 $mL \cdot min^{-1}$, relative standard deviation < 0.5%). In theory, the lower the flow rate of the HPLC pump is, the longer residence time will be realized. However, the experiments showed that it was difficult for the HPLC pump to continue working with the very low flow rate (approximately less than 3 $mL \cdot min^{-1}$) and high pressure (above critical pressure of water). Therdthianwong *et al*. (2011) reported that ethanol conversion can reach 97.3 wt% at 550 °C with approximately 50 s. Further, due to the effective residence time

range of glucose decomposition (6.1 s to 12.9 s), the residence time range of 6 s to 12 s was selected

Figure 3 indicates that the *GE* values and the yields of H_2, CO, and C_2 obviously decreased as residence time increased from 6 s to 12 s at 550 °C.

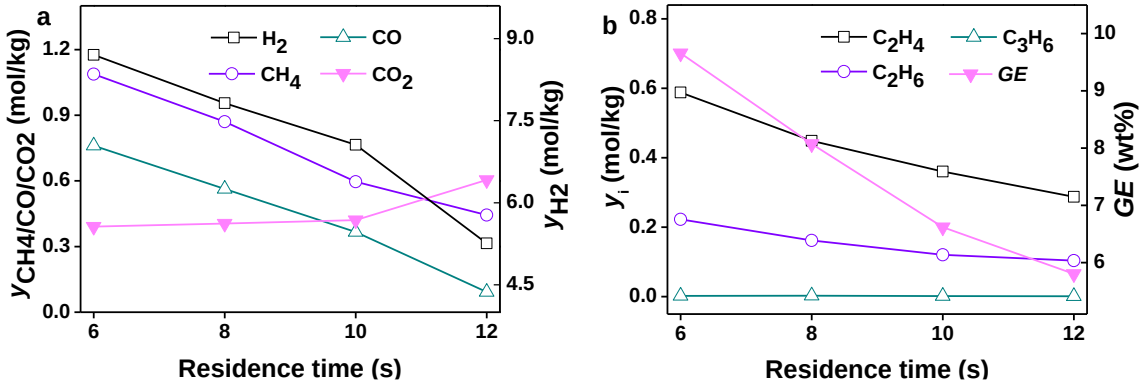

Fig. 3. Gas product yield and *GE* at different residence times (reaction temperature: 550 °C, reaction pressure: 23 MPa, and $[C_2H_5OH]_0$: 0.1 mol/L): (a) H_2, CH_4, CO, and CO_2; (b) C_2H_4, C_2H_6, C_3H_6, and *GE*

The water-gas shift reaction (Eq. 6) is an important reaction route in supercritical water. When the forward reaction occurs, which is favored from 6 s to 12 s, CO will continue being consumed. In addition, several studies have reported that CO (Eq. 7 and Eq. 8), C_2 (Eq. 9), CH_4 (Eq. 10), and CO_2 (Eq. 11) can be reduced by the coke production resulting from cracking reactions (Therdthianwong *et al*. 2011; Reddy *et al*. 2014). As residence time increased (Fig. 3a), the CO_2 yield obviously increased, which indicates that CO_2 methanation (Miao *et al*. 2016) was not the dominant route under these reaction conditions. Moreover, from 6 s to 12 s, H_2 may be reduced by a hydrogenation reaction (such as Eq. 12 (Castello and Fiori 2012)). Equations 6 through 10 are as follows:

$$CO+H_2O \leftrightarrow CO_2+H_2 \quad (6)$$

$$CO \rightarrow C+0.5O_2 \quad (7)$$

$$2CO \rightarrow C+CO_2 \quad (8)$$

$$C_2H_4 \rightarrow 2C+2H_2 \quad (9)$$

$$CH_4 \rightarrow C+2H_2 \quad (10)$$

$$CO_2+2H_2 \rightarrow C+2H_2O \quad (11)$$

$$CHO\cdot+H_2 \rightarrow CH_2OH\cdot \quad (12)$$

According to previously postulated reaction pathways (Therdthianwong *et al*. 2011; Chakinala *et al*. 2013), it can be inferred that C_3H_6 was produced by 2-propanol dehydration (Eq. 13), the C=O cleavage of acetone (Eq. 14), and C_2H_4 hydrogenation (Eq. 3). Figure 3(b) shows that at 6 s to 12 s, the C_3H_6 yield kept at quite low value. Thus, the reaction rates of Eq. 3, Eq. 13, and Eq. 14 were relatively small.

$$(CH_3)_2CHOH \rightarrow C_3H_6+H_2O \quad (13)$$

$$CH_3COCH_3 \rightarrow C_3H_6+O\cdot \quad (14)$$

Maximum hydrogen yield *via* supercritical water gasification commonly requires sufficient residence time for the complete conversion of long-living intermediates (even up to 120 min (Okolie *et al*. 2019)). Because many intermediates have been considered as short-living components during the feedstock decomposition process (Kruse *et al*. 2010), the experiments of this study were conducted with 6 s to 12 s residence times to better reveal the conversion mechanism of the organic compounds.

Feedstock Concentration

Feedstock concentration is an important operational parameter for biomass gasification in supercritical water (Pinkard *et al*. 2018). In industrial applications, higher feedstock concentration is beneficial to production efficiency. With higher feedstock concentrations, more hydrogen is provided (in theory), which is good for hydrogen production. In addition, higher feedstock concentration means a decrease in water content. The water-gas shift reaction (Eq. 6) plays an important role in the hydrogen production process (LeValley *et al*. 2014). High feedstock concentration may result in reduced hydrogen production (Okolie *et al*. 2019). Figure 4 shows that the initial ethanol concentration was set at 0.05 to 0.20 mol·L^{-1} (less than 1 wt% by mass concentration). Figure 4 shows that the gas product yields clearly increased with higher feedstock concentrations, except for C_3H_6. According to the water-gas shift forward reaction ($CO+H_2O \rightarrow CO_2+H_2$), the H_2-to-CO_2 ratio should be 1. However, in Fig. 4a, the yield of H_2 was far beyond that of the other gas products, especially at the higher feedstock concentration. This was because ethanol dehydrogenation (Eq. 1) was the initial pathway for ethanol decomposition, and a large amount of acetaldehyde was detected during ethanol decomposition process by Abdullah and Croiset (2014). Resende and Savage (2010) also reported that a residence time of 12 s was far from the equilibrium of the water-gas shift reaction. Thus, the H_2 yield was greater than the CO_2 yield (Fig. 4a), and the H_2-to-CO_2 ratio increased as the initial ethanol concentration increased. Because C_2H_4 was mainly produced by ethanol dehydration (Abdullah and Croist 2014) (Fig. 4b), the higher feedstock concentration facilitated the ethanol dehydration reaction. Further, because the C_2H_4 yield was increased at the high feedstock concentration, more C_2H_6 was formed by C_2H_4 hydrogenation (Therdthianwong *et al*. 2011; Okolie *et al*. 2019). In addition, Fig. 4a shows that the related pathways of C_3H_6 (Eqs. 13 and 14) were not the dominant reactions during the ethanol decomposition, even at 0.20 mol·L^{-1}.

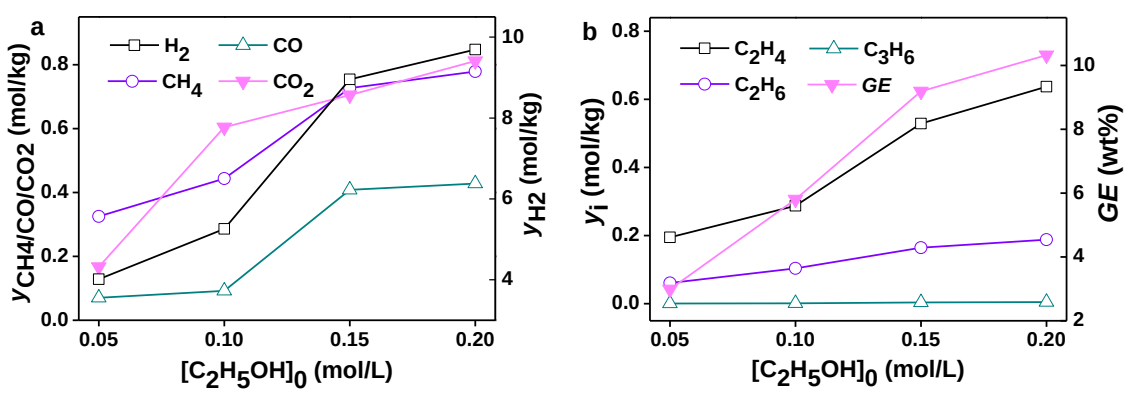

Fig. 4. Gas product yield and *GE* at different feedstock concentrations (reaction temperature: 550 °C, reaction pressure: 23 MPa, and residence time: 12 s): (a) H_2, CH_4, CO, and CO_2; (b) C_2H_4, C_2H_6, C_3H_6, and *GE*

Kinetics Analysis

The products of ethanol gasification in supercritical water included the gas phase (H_2, CO, CO_2, CH_4, C_2H_6, C_2H_4, and C_3H_6), liquid phase (acetaldehyde, acetone, 2-propanol, *etc.* (Chakinala *et al*. 2013)), and some coke. According to the above discussion, the ethanol decomposition mechanism is summarized in Fig. 5. In Fig. 5, 2-propanol, acetone, *etc.* (defined as INT_1) were formed by ethanol direct conversion. Because acetaldehyde is the main intermediate compound in the liquid phase during ethanol decomposition (Therdthianwong *et al*. 2011; Abdullah and Croiset 2014), the formation and degradation of acetaldehyde should be the important pathways of ethanol supercritical water decomposition (as shown in Fig. 5). In addition, Tschannen *et al*. (2013) reported that the acetaldehyde process produced long-chain aldehydes, such as propionaldehyde, butyraldehyde, pentanaldehyde, *etc*. Thus, these long-chain aldehydes were named INT_2. The gas production (ethanol direct decomposition and the further conversion of the intermediates) and gas mutual conversion processes (water-gas shift reaction, methanation, and hydrogenation) were defined as "Gases" in Fig. 5. The coke formation derived from the gas products is also depicted in Fig. 5. It has to be pointed out that Figure 5 was a simplified reaction network of ethanol decomposition, and the detailed pathways were not thoroughly shown in Fig. 5.

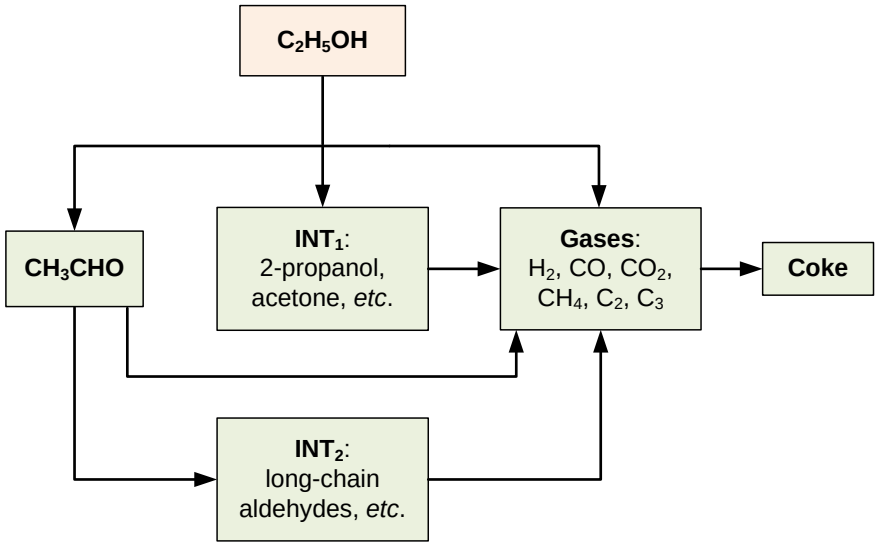

Fig. 5. Proposed simplified decomposition mechanism for ethanol in supercritical water

The experiments showed that the C_3H_6 yield was only 0.003 mol·kg^{-1} at 550 °C and 23 MPa. Therefore, the gas products of ethanol gasification in the kinetic model were simplified as H_2, CO, CO_2, CH_4, C_2H_4, and C_2H_6. With regard to the liquid products of ethanol decomposition, some related studies (Arita *et al*. 2003; Therdthianwong *et al*. 2011; Abdullah and Croiset 2014; Reddy *et al*. 2014) have reported that acetaldehyde was the main component. Therefore, the liquid products in this kinetic model were classified as acetaldehyde and other intermediates (defined as $C_xH_yO_z$). In addition, according to the results in Fig. 3, the coke formation and hydrogenation of the intermediates should be included in the kinetic model. Further, because the H_2-to-CO_2 ratios (Fig. 2, Fig. 3, and Fig. 4) exceeded 1, the water-gas shift reaction can be ignored in the kinetics. Methanation is the exothermic reaction, and the favorable reaction temperature of methanation is less than

400 °C (Miao *et al*. 2016). Guo *et al.* (2014) found that the methanation reaction can be excluded in the kinetic model for temperatures from 550 °C to 600 °C. As a result, a kinetic model of ethanol gasification in supercritical water is shown in Table 1.

Table 1. Proposed Reaction Pathways of Ethanol Decomposition in Supercritical Water

Reaction	k_i (Forward Reaction)	k_{-i} (Reverse Reaction)	Index
$C_2H_5OH \rightarrow CH_3CHO + H_2$	k_1	*	(1)
$C_2H_5OH \rightarrow C_2H_4 + H_2O$	k_2	*	(2)
$C_2H_4 + H_2 \leftrightarrow C_2H_6$	k_3	k_{-3}	(3)
$CH_3CHO \rightarrow CH_4 + CO$	k_4	*	(15)
$2CO \rightarrow C + CO_2$	k_5	*	(8)
$C_2H_4 \rightarrow 2C + 2H_2$	k_6	*	(9)
$CH_4 \rightarrow C + 2H_2$	k_7	*	(10)
$CO_2 + 2H_2 \rightarrow C + 2H_2O$	k_8	*	(11)
$C_xH_yO_z + H_2 \rightarrow C_xH_{y+2}O_z$	k_9	*	(16)
Note: * = ignored			

According to the kinetic model in Table 2, the reaction rate equations with the first-order were expressed as Eq. 17 to Eq. 25. When the reaction rate constants of Eq. 17 to Eq. 25 were solved, the reaction kinetic process was comprehensively revealed:

$$\frac{\mathrm{d}C_{\mathrm{H_2}}}{\mathrm{d}t} = k_1 C_{\mathrm{C_2H_5OH}} - k_3 C_{\mathrm{C_2H_4}} C_{\mathrm{H_2}} + k_{-3} C_{\mathrm{C_2H_6}} + 2k_6 C_{\mathrm{C_2H_4}} + 2k_7 C_{\mathrm{CH_4}} - 2k_8 C_{\mathrm{CO_2}} C_{\mathrm{H_2}} - k_9 C_{\mathrm{C_xH_yO_z}} C_{\mathrm{H_2}} \tag{17}$$

$$\frac{\mathrm{d}C_{\mathrm{CO}}}{\mathrm{d}t} = k_4 C_{\mathrm{CH_3CHO}} - 2k_5 C_{\mathrm{CO}} \tag{18}$$

$$\frac{\mathrm{d}C_{\mathrm{CO_2}}}{\mathrm{d}t} = k_5 C_{\mathrm{CO}} - k_8 C_{\mathrm{CO_2}} C_{\mathrm{H_2}} \tag{19}$$

$$\frac{\mathrm{d}C_{\mathrm{CH_4}}}{\mathrm{d}t} = k_4 C_{\mathrm{CH_3CHO}} - k_7 C_{\mathrm{CH_4}} \tag{20}$$

$$\frac{\mathrm{d}C_{\mathrm{C_2H_4}}}{\mathrm{d}t} = k_2 C_{\mathrm{C_2H_5OH}} - k_3 C_{\mathrm{C_2H_4}} C_{\mathrm{H_2}} + k_{-3} C_{\mathrm{C_2H_6}} - k_6 C_{\mathrm{C_2H_4}} \tag{21}$$

$$\frac{\mathrm{d}C_{\mathrm{C_2H_6}}}{\mathrm{d}t} = k_3 C_{\mathrm{C_2H_4}} C_{\mathrm{H_2}} - k_{-3} C_{\mathrm{C_2H_6}} \tag{22}$$

$$\frac{\mathrm{d}C_{\mathrm{C_2H_5OH}}}{\mathrm{d}t} = -\left(k_1 + k_2\right) C_{\mathrm{C_2H_5OH}} \tag{23}$$

$$\frac{\mathrm{d}C_{\mathrm{C}}}{\mathrm{d}t} = k_5 C_{\mathrm{CO}} + 2k_6 C_{\mathrm{C_2H_4}} + k_7 C_{\mathrm{CH_4}} + k_8 C_{\mathrm{CO_2}} C_{\mathrm{H_2}} \tag{24}$$

$$\frac{\mathrm{d}C_{\mathrm{CH_3CHO}}}{\mathrm{d}t} = k_1 C_{\mathrm{C_2H_5OH}} - k_4 C_{\mathrm{CH_3CHO}} \tag{25}$$

Based on the data in the "Residence Time" section and the least-square-fit method using Micromath Scientist, the rate constants of Eq. 17 to Eq. 25 were solved, and the results are shown in Table 2. It was found that ethanol gasification in supercritical water was mainly dominated by ethanol dehydrogenation (k_1), intermediate hydrogenation (k_9), and coke formation (k_5 and k_7). Figure 6 shows that the H_2 concentration of the kinetic model well predicted the results of the experiments (R^2 = 0.9136). Because the aim of supercritical water gasification is often hydrogen production (Correa and Kruse 2018), the rates of H_2 formation and consumption are shown in Fig. 7.

Table 2. Reaction Rate Constant (k_i, s^{-1}) Values

k_i	Value	k_i	Value
k_1	0.2157	k_5	1.9380E-2
k_2	4.7702E-3	k_6	5.6309E-16
k_3	6.6029E-16	k_7	1.8039E-2
k_{-3}	6.7517E-16	k_8	1.8107E-16
k_4	7.3274E-3	k_9	0.1743

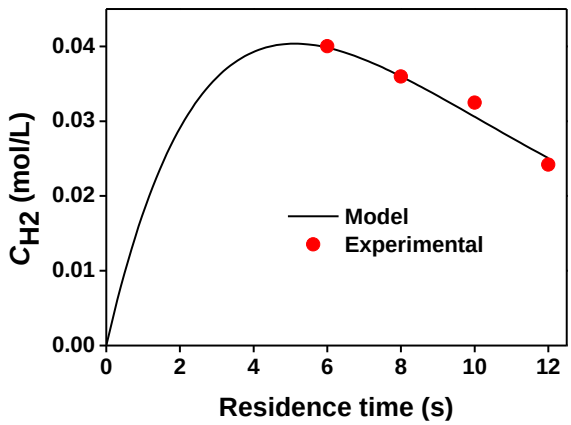

Fig. 6. The H_2 concentrations of the kinetic model and the experiment (reaction temperature: 550 °C, reaction pressure: 23 MPa, $[C_2H_5OH]_0$: 0.1 mol/L, and residence time: 6 s to 12 s)

Figure 7 shows that H_2 was mainly formed *via* the ethanol dehydrogenation pathway, and it was consumed *via* hydrogenation of the intermediates.

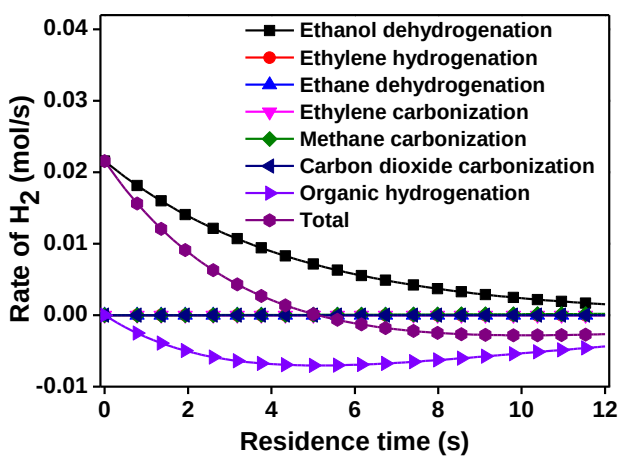

Fig. 7. Rates of H_2 formation and consumption (reaction temperature: 550 °C, reaction pressure: 23 MPa, and $[C_2H_5OH]_0$: 0.1 mol/L)

In addition, Arita *et al.* (2003) reported that ethanol dehydrogenation was the initial decomposition reaction of ethanol with a relatively fast reaction rate. As residence time increased, the rate of H_2 formation *via* ethanol dehydrogenation gradually decreased (Fig. 7), which was due to ethanol degradation by dehydration (Eq. 2). Figure 7 shows that the rates of H_2 formation *via* carbonization pathways were not sufficiently fast. Therefore, coke formation during the ethanol decomposition process was limited. In summary, the proposed reaction pathways of ethanol decomposition in supercritical water and its kinetic model (Table 1) preliminarily revealed the ethanol decomposition mechanism.

CONCLUSIONS

1. The gas products of ethanol decomposition in supercritical water were mainly H_2, CO, CO_2, CH_4, and C_2 (C_2H_6 and C_2H_4), and the C_3H_6 yield was limited.
2. Temperature had bigger impacts on gas production than the other factors. The gas yields and gasification efficiency increased with the increases in temperature and feedstock concentration. The higher reaction temperature was beneficial to ethanol gasification in supercritical water by promoting the free-radical reactions. The C-C bond and C-O bond scissions of ethanol were favored by the high reaction temperature. The favorable temperature for ethanol decomposition should be above 550 °C to achieve high gasification efficiency.
3. As the feedstock concentration increased from 0.05 $mol \cdot L^{-1}$ to 0.20 $mol \cdot L^{-1}$, the H_2-to-CO_2 ratio and the C_2H_4 yield gradually increased, and the H_2-to-CO_2 ratio was much greater than 1. Higher feedstock concentration facilitated ethanol dehydrogenation and ethanol dehydration. In addition, the water-gas shift reaction can be ignored in the kinetic model.
4. As residence time increased, the *GE* values and the yields of H_2, CO, and C_2 obviously decreased, whereas the CO_2 yield slightly increased. When the residence time increased from 6 s to 12 s, the H_2 amount may have been reduced by the hydrogenation reaction, and CO_2 methanation was not the dominant reaction. Moreover, the coke formation pathways should be included in the kinetic model of the ethanol decomposition.
5. A kinetic model of ethanol supercritical water decomposition was established based on the above results. It showed that ethanol gasification in supercritical water was mainly dominated by ethanol dehydrogenation, the hydrogenation of intermediates, and the coke formation of CO and CH_4. In addition, H_2 was mainly formed *via* the ethanol dehydrogenation pathway, and it was consumed *via* the hydrogenation of intermediates. As residence time increased, the rate of H_2 formation *via* ethanol dehydrogenation gradually decreased because of the competing dehydration reaction of ethanol. Coke formation was limited during ethanol decomposition in supercritical water.

ACKNOWLEDGMENTS

This research was financially supported by the National Natural Science Foundation of China (No. 51606103) and the Opening Research Fund Program of the Key Laboratory of Energy Thermal Conversion and Control of the Ministry of Education of

Southeast University (No. 2016007). The authors acknowledge the support of the Advanced Analysis and Testing Center of Nanjing Forestry University.

REFERENCES CITED

Abdullah, T. A. T., and Croiset, E. (2014). "Evaluation of an inconel-625 reactor and its wall effects on ethanol reforming in supercritical water," *Industrial & Engineering Chemistry Research* 53(6), 2121-2129. DOI: 10.1021/ie403305d

Arita, T., Nakahara, K., Nagami, K., and Kajimoto, O. (2003). "Hydrogen generation from ethanol in supercritical water without catalyst," *Tetrahedron Letters* 44(5), 1083-1086. DOI: 10.1016/S0040-4039(02)02704-1

Boukis, N., Diem, V., Galla, U., and Dinjus, E. (2006). "Methanol reforming in supercritical water for hydrogen production," *Combustion Science and Technology* 178(1-3), 467-485. DOI: 10.1080/00102200500292316

Castello, D., and Fiori, L. (2012). "Kinetics modeling and main reaction schemes for the supercritical water gasification of methanol," *Journal of Supercritical Fluids* 69, 64-74. DOI: 10.1016/j.supflu.2012.05.008

Castello, D., Kruse, A., and Fiori, L. (2015). "Low temperature supercritical water gasification of biomass constituents: Glucose/phenol mixtures," *Biomass & Bioenergy* 73, 84-94. DOI: 10.1016/j.biombioe.2014.12.010

Chakinala, A. G., Kumar, S., Kruse, A., Kersten, S. R. A., Swaaij, W. P. M. V., and Brilman, D. W. F. (2013). "Supercritical water gasification of organic acids and alcohols: The effect of chain length," *The Journal of Supercritical Fluids* 74, 8-21. DOI: 10.1016/j.supflu.2012.11.013

Correa, C. R., and Kruse, A. (2018). "Supercritical water gasification of biomass for hydrogen production – Review," *The Journal of Supercritical Fluids* 133(Part 2), 573-590. DOI: 10.1016/j.supflu.2017.09.019

Durak, H. (2015). "Thermochemical conversion of phellinus pomaceus via supercritical fluid extraction and pyrolysis processes," *Energy Conversion and Management* 99, 282-298. DOI: 10.1016/j.enconman.2015.04.050

Durak, H. (2018). "*Trametes versicolor* (L.) mushrooms liquefaction in supercritical solvents: Effects of operating conditions on product yields and chromatographic characterization," *The Journal of Supercritical Fluids* 131, 140-149. DOI: 10.1016/j.supflu.2017.09.013

Genel, Y., Durak, H., Aysu, T., and Genel, I. (2016). "Effect of process parameters on supercritical liquefaction of xanthium strumarium for bio-oil production," *The Journal of Supercritical Fluids* 115, 42-53. DOI: 10.1016/j.supflu.2016.04.009

Guo, S., Guo, L., Cao, C., Yin, J., Lu, Y., and Zhang, X. (2012). "Hydrogen production from glycerol by supercritical water gasification in a continuous flow tubular reactor," *International Journal of Hydrogen Energy* 37(7), 5559-5568. DOI: 10.1016/j.ijhydene.2011.12.135

Guo, Y., Wang, S., Huelsman, C. M., and Savage, P. E. (2014). "Kinetic model for reactions of indole under supercritical water gasification conditions," *Chemical Engineering Journal* 241, 327-335. DOI: 10.1016/j.cej.2013.11.012

Hack, W., Masten, D. A., and Buelow, S. J. (2005). "Methanol and ethanol decomposition in supercritical water," *Zeitschrift für Physikalische Chemie* 219(3), 367-378. DOI: 10.1524/zpch.219.3.367.59179

Holgate, H. R., Meyer, J. C., and Tester, J. W. (1995). "Methanol and ethanol decomposition in supercritical water," *AIChE Journal* 41(3), 637-648. DOI: 10.1002/aic.690410320

Kruse, A., and Gawlik, A. (2003). "Biomass conversion in water at 330-410 °C and 30-50 MPa. Identification of key compounds for indicating different chemical reaction pathways," *Industrial & Engineering Chemistry Research* 42(2), 267-279. DOI: 10.1021/ie0202773

Kruse, A., Bernolle, P., Dahmen, N., Dinjus, E., and Maniam, P. (2010). "Hydrothermal gasification of biomass: Consecutive reactions to long-living intermediates," *Energy and Environmental Science* 3(1), 136-143. DOI: 10.1039/B915034J

Lee, I.-G., Kim, M.-S., and Ihm, S.-K. (2002). "Gasification of glucose in supercritical water," *Industrial & Engineering Chemistry Research* 41(5), 1182-1188. DOI: 10.1021/ie010066i

LeValley, T. L., Richard, A. R., and Fan, M. (2014). "The progress in water gas shift and steam reforming hydrogen production technologies – A review," *International Journal of Hydrogen Energy* 39(30), 16983-17000. DOI: 10.1016/j.ijhydene.2014.08.041

Mesa, L., Martinez, Y., de Armas, A. C., and Gonzalez, E. (2020). "Ethanol production from sugarcane straw using different configurations of fermentation and techno-economical evaluation of the best schemes," *Renewable Energy* 156, 377-388. DOI: 10.1016/j.renene.2020.04.091

Miao, B., Ma, S. S. K., Wang, X., Su, H., and Chan, S. H. (2016). "Catalysis mechanisms of CO_2 and CO methanation," *Catalysis Science & Technology* 6(12), 4048-4058. DOI: 10.1039/C6CY00478D

Okolie, J. A., Rana, R., Nanda, S., Dalai, A. K., and Kozinski, J. A. (2019). "Supercritical water gasification of biomass: A state-of-the-art review of process parameters, reaction mechanisms and catalysis," *Sustainable Energy and Fuels* 3(3), 578-598. DOI: 10.1039/C8SE00565F

Pinkard, B. R., Gorman, D. J., Tiwari, K., Kramlich, J. C., Reinhall, P. G., and Novosselov, I. V. (2018). "Review of gasification of organic compounds in continuous-flow, supercritical water reactors," *Industrial & Engineering Chemistry Research* 57(10), 3471-3481, DOI: 10.1021/acs.iecr.8b00068

Pinkard, B. R., Rasmussen, E. G., Kramlich, J. C., Reinhall, P. G., and Novosselov, I. V. (2019). "Supercritical water gasification of ethanol for fuel gas production," in: *Proceedings of the ASME 13th International Conference on Energy Sustainability*, Bellevue, WA, USA, Article number 3950. DOI: 10.1115/ES2019-3950

Reddy, S. N., Nanda, S., Dalai, A. K., and Kozinski, J. A. (2014). "Supercritical water gasification of biomass for hydrogen production," *International Journal of Hydrogen Energy* 39(13), 6912-6926. DOI: 10.1016/j.ijhydene.2014.02.125

Reddy, S. N., Nanda, S., and Kozinski, J. A. (2016). "Supercritical water gasification of glycerol and methanol mixtures as model waste residues from biodiesel refinery," *Chemical Engineering Research & Design* 113, 17-27. DOI: 10.1016/j.cherd.2016.07.005

Resende, F. L. P., and Savage, P. E. (2010). "Kinetic model for noncatalytic supercritical water gasification of cellulose and lignin," *AIChE Journal* 56(9), 2412-2420. DOI: 10.1002/aic.12165

Sangwan, M., Yan, C., Chesnokov, E. N., and Krasnoperov, L. N. (2015). "Reaction CH_3 + CH_3 -> C_2H_6 studied over the 292-714 K temperature and 1-100 bar pressure

ranges," *Journal of Physical Chemistry A* 119(28), 7847-7857. DOI: 10.1021/acs.jpca.5b01276

Sato, O., Yamaguchi, A., Murakami, Y., Takahashi, T., Enda, Y., and Shirai, M. (2013). "Supercritical water gasification of residue from ethanol production from Japanese cedar," *Energy & Fuels* 27(7), 3861-3866. DOI: 10.1021/ef400753x

Therdthianwong, S., Srisiriwat, N., Therdthianwong, A., and Croiset, E. (2011). "Hydrogen production from bioethanol reforming in supercritical water," *Journal of Supercritical Fluids* 57(1), 58-65. DOI: 10.1016/j.supflu.2011.02.005

Tschannen, R., Gonzales, A., and Lee, S. (2013). "Chemical reactions of formaldehyde and acetaldehyde in supercritical water," *Energy Technology* 1(5-6), 350-358. DOI: 10.1002/ente.201300034

Watanabe, M., Sato, T., Inomata, H., Smith, R. L., Arai, K., Kruse, A., and Dinjus, E. (2004). "Chemical reactions of C_1 compounds in near-critical and supercritical water," *Chemical Reviews* 104(12), 5803-5822. DOI: 10.1021/cr020415y

Yan, C., and Krasnoperov, L. N. (2019). "Pressure-dependent kinetics of the reaction between CH_3O_2 and OH: TRIOX formation," *Journal of Physical Chemistry A* 123(39), 8349-8357. DOI: 10.1021/acs.jpca.9b03861

Zhao, L. (2013). *Study on Effects of Potassium Existing in Biomass on Small Molecule Intermediates Gasification Conversion in Supercritical Water*, Ph.D. Dissertation, Southeast University, Nanjing, China.

Zhao, L., Zhou, H., Yin, Y., Lu, Q., and Zhang, J. (2020). "Effects of potassium carbonate on acetaldehyde gasification in supercritical water," *Energy Sources, Part A: Recovery, Utilization, and Environmental Effects* 42(10), 1286-1298. DOI: 10.1080/15567036.2019.1648602

Article submitted: August 23, 2020; Peer review completed: September 13, 2020; Revised version received and accepted: September 18, 2020; Published: September 23, 2020.
DOI: 10.15376/biores.15.4.8515-8528